

# High Precision Variational Bayesian Inference of Sparse Linear Networks <sup>★</sup>

Junyang Jin <sup>a</sup>, Ye Yuan <sup>b,★</sup>, and Jorge Gonçalves <sup>a</sup>

<sup>a</sup>*The Luxembourg Centre for Systems Biomedicine, avenue du Swing, 4367 Belvaux, Luxembourg*

<sup>b</sup>*School of Automation, Huazhong University of Science and Technology, 430074, Hubei, China*

---

## Abstract

Sparse networks can be found in a wide range of applications, such as biological and communication networks. Inference of such networks from data has been receiving considerable attention lately, mainly driven by the need to understand and control internal working mechanisms. However, while most available methods have been successful at predicting many correct links, they also tend to infer many incorrect links. Precision is the ratio between the number of correctly inferred links and all inferred links, and should ideally be close to 100%. For example, 50% precision means that half of inferred links are incorrect, and there is only a 50% chance of picking a correct one. In contrast, this paper develops a method, based on variational Bayesian inference and Gaussian processes, that focuses on inferring links with very high precision. In addition, our method does not require full-state measurements and effectively promotes both system stability and network sparsity. Monte Carlo simulations illustrate that our method has 100% or nearly 100% precision, even in the presence of noise. The method should be applicable to a wide range of network inference contexts, including biological networks and power systems.

*Key words:* System Identification; Variational Inference; Dynamical Structure Function; Network Inference; Sparse Networks

---

## 1 INTRODUCTION

In systems biology, mathematical modelling has been central to the study of biological networks. Dynamical models are frequently developed to predict the behaviour of systems in response to external or internal stimulus for example, drug treatment or mutation. Yet only input-output dynamics are learned without exploring the topology, whereas in many other applications, comprehensive knowledge of the network topology is required. For example, the information about the structure of control systems is essential for fault diagnosis. Hence, both the inference of system dynamics and the detection of network topology are important.

Sparsity and stability are fundamental properties of most real-world networks. Biological networks are naturally stable and tend to be sparse: typically, a molecule will bind with a small number of other molecules. Communication networks, as artificial systems, are designed to be stable for robust operation and sparse to reduce the time delay of signal transmission and energy consumption. Thus, sparsity and stability are primary constraints in network inference, especially in the case of limited data source or high amount of noise.

When dealing with practical networks, a typical problem is incomplete data collection. Often, because of either high experimental cost or technical limitations, not all the nodes in the network can be measured. Moreover, it is common that neither the number of hidden nodes nor their internal connectivity are known. The difficulty here is that many inference methods nonetheless assume full-state measurements. It is important to reconsider this issue carefully.

Precision is the first priority when solving network inference. With low precision, inferred networks cannot be trusted. However, most state-of-the-art methods can rarely achieve 100% precision, meaning that not all inferred links are correct. The motivation of this work is to develop a method that offers 100% or nearly 100% precision.

In recent years, kernel-based methods have become popular in the system identification community [23]. For linear systems, the methods effectively impose system stability and greatly simplify the estimation of model complexity. Kernel-based methods have successfully identified SISO continuous linear time invariant (LTI) models [23] and been further extended to discrete LTI systems [5, 8, 23]. In particular, kernel-based methods have been used to infer sparse networks described by Granger causality [9]. In addition, system identification of a vari-

---

<sup>★</sup> For correspondence: yye@hust.edu.cn.

ety of model classes have been considered: the models include NFI, NARX, NARMAX, linear parameter-varying (LPV) Box-Jenkins models, Hammerstein models, and cascaded linear systems [11, 25, 27, 28]. System dynamics and network topology are controlled by the hyperparameters of kernel functions. Under the Bayesian paradigms, kernel-based methods apply empirical Bayes to estimate hyperparameters (KEB). By incorporating Automatic Relevance Determination (ARD), kernel-based methods are able to enforce sparsity, where the sparsity profile of the solution implies network topology [5, 9]. Nevertheless, this framework is not ideal for topology detection. Due to local optimal solutions, it is very difficult to achieve 100% precision.

Variational inference (VI), as empirical Bayes, is a Bayesian deterministic approximation technique that has been applied to a number of cases, including sparse regression models [1, 31] and neural networks [2, 14, 18]. Instead of estimating hyperparameters directly, VI searches for an approximation of the posterior distribution of hyperparameters (functional estimation). With well-posed models of exponential families, VI is as efficient computationally as empirical Bayes and can be much more accurate [15, 16]. More importantly, VI is able to estimate model evidence for each possible model structure: this enables evaluation of the relative confidence between models. Nevertheless, VI is barely used in kernel-based system identification. Due to the nonlinearity introduced by kernel functions (non-gaussianity), VI no longer holds a closed-form update in the algorithm and has to deal with high-dimensional ill-conditioned covariance matrices, which seriously increases computational burden and degrades numerical stability.

This paper combines Gaussian processes and VI to infer sparse networks. Dynamical structure functions are used to describe sparse linear networks where the information of hidden nodes is encoded via transfer functions. By expressing DSF models in a non-parametric way, the system can be identified without knowing the number of hidden nodes and the connectivity among them. VI is employed to identify system dynamics and infer network topology. Thanks to the recent development on the analysis of kernel functions, VI is implemented in a more efficient and robust way by using a special kernel function (Tuned/Correlated kernel). More importantly, by applying the backward selection strategy, the proposed method encourages high inference precision. Monte Carlo simulations show that our method produces more reliable networks than KEB under various experimental conditions, such as different topologies, noise levels, kernel functions and number of data points. Most importantly, the proposed method always achieves 100% or nearly 100% precision so that all inferred links are correct.

The paper is organized as follows. Section 2 introduces variational inference algorithms. Section 3 introduces dynamical structure function and formulates the full Bayesian model. Section 4 discusses network inference using variational inference. Section 5 compares the

method with other approaches via Monte Carlo simulations. Finally, Section 6 concludes and discusses further development in this field.

*Notation:* The notation in this paper is as follows.  $I_n$  denotes a  $n \times n$  identity matrix. For  $L \in R^{n \times n}$ ,  $diag\{L\}$  denotes a vector which consists of the diagonal elements of matrix  $L$ .  $[L]_{ij}$  presents the  $ij$ th entry and  $\bar{L}_i^j$  denotes the  $i$ th  $j \times j$  diagonal block of  $L$ . For a series of matrices,  $\{L_i | i = 1, \dots, n\}$ ,  $blkdiag\{L_1, \dots, L_n\}$  denotes a block diagonal matrix. For  $l \in R^n$ ,  $diag\{l\}$  denotes a diagonal matrix whose diagonal elements come from vector  $l$ .  $l_{ij}$  denotes the  $j$ th element of the  $i$ th group of  $l$ . A vector,  $y(t_1 : t_2)$  denotes a row vector  $[y(t_1) \ y(t_1 + 1) \ \dots \ y(t_2)]$ .  $\mathcal{N}(x|m, \Sigma)$  denotes a Gaussian distribution of  $x$  with mean  $m$  and covariance matrix  $\Sigma$ .  $asc\{a_1, \dots, a_n\}$  means to rearrange the elements in an ascending order of the magnitude.

## 2 OVERVIEW OF VI

Variational inference approximates a full Bayesian model analytically so that the intractable marginalization or expectation can be easily calculated [19, 32]. Empirical Bayes was more frequently used in the kernel-based system identification, where system dynamics is the main concern. Under the context of network inference, model selection (detection of network topology) is another important aspect. Whilst model evidence is usually required to compare different model structures, empirical Bayes cannot provide a good approximation. In contrast, variational inference generates a lower bound of model evidence, which motivates more advanced strategies for model selection. Consider a model structure  $\mathcal{M}_k$  with model parameters,  $\theta$ . The model evidence,  $p(y|\mathcal{M}_k)$  is expressed as:

$$p(y|\mathcal{M}_k) = \int p(y|\theta, \mathcal{M}_k)p(\theta|\mathcal{M}_k)d\theta. \quad (1)$$

Assuming an arbitrary distribution  $Q(\theta|\mathcal{M}_k)$  is used to approximate  $p(\theta|y, \mathcal{M}_k)$ , we have:

$$\begin{aligned} \ln p(y|\mathcal{M}_k) &= \ln \frac{p(y|\theta, \mathcal{M}_k)p(\theta|\mathcal{M}_k)}{p(\theta|y, \mathcal{M}_k)} \\ &= \int Q(\theta|\mathcal{M}_k) \ln \frac{p(y|\theta, \mathcal{M}_k)p(\theta|\mathcal{M}_k)}{p(\theta|y, \mathcal{M}_k)} d\theta \\ &= \int Q(\theta|\mathcal{M}_k) \ln \frac{p(y|\theta, \mathcal{M}_k)p(\theta|\mathcal{M}_k)}{Q(\theta|\mathcal{M}_k)} d\theta \\ &+ \int Q(\theta|\mathcal{M}_k) \ln \frac{Q(\theta|\mathcal{M}_k)}{p(\theta|y, \mathcal{M}_k)} d\theta \\ &= L[Q(\theta|y, \mathcal{M}_k)] + KL[Q(\theta|\mathcal{M}_k)||p(\theta|y, \mathcal{M}_k)]. \end{aligned} \quad (2)$$

where

$$L[Q(\theta|y, \mathcal{M}_k)] = \int Q(\theta|\mathcal{M}_k) \ln \frac{p(y|\theta, \mathcal{M}_k)p(\theta|\mathcal{M}_k)}{Q(\theta|\mathcal{M}_k)} d\theta$$

$$KL[Q(\theta|\mathcal{M}_k)||p(\theta|y, \mathcal{M}_k)] = \int Q(\theta|\mathcal{M}_k) \ln \frac{Q(\theta|\mathcal{M}_k)}{p(\theta|y, \mathcal{M}_k)} d\theta. \quad (3)$$

The second term of (2) is the Kullback-Leibler (KL) divergence between  $Q(\theta|\mathcal{M}_k)$  and  $p(\theta|y, \mathcal{M}_k)$ . KL divergence is non-negative and equal to zero if and only if  $Q(\theta|\mathcal{M}_k) = p(\theta|y, \mathcal{M}_k)$ . Therefore, KL divergence measures the difference between the true and the approximate distributions. More importantly, since  $KL[Q(\theta|\mathcal{M}_k)||p(\theta|y, \mathcal{M}_k)] \geq 0$ ,  $\ln p(y|\mathcal{M}_k) \geq L[Q(\theta|y, \mathcal{M}_k)]$ , meaning  $L[Q(\theta|y, \mathcal{M}_k)]$  is the lower bound of the logarithm of model evidence. Hence, it can be used as an approximation of model evidence for model selection.

VI employs KL divergence as the metric to measure the accuracy of the approximation. Therefore, the goal is to find the optimal  $Q(\theta|y, \mathcal{M}_k)$  that minimizes the KL divergence:

$$Q_{opt}(\theta|y, \mathcal{M}_k) = \arg \min_Q KL[Q(\theta|\mathcal{M}_k)||p(\theta|y, \mathcal{M}_k)]. \quad (4)$$

According to (2), the optimization problem is equivalent to maximizing the lower bound  $L[Q(\theta|y, \mathcal{M}_k)]$ :

$$Q_{opt}(\theta|y, \mathcal{M}_k) = \arg \max_Q L[Q(\theta|y, \mathcal{M}_k)]. \quad (5)$$

Without further constraints on  $Q(\theta|y, \mathcal{M}_k)$ , the solution is  $Q(\theta|y, \mathcal{M}_k) = p(\theta|y, \mathcal{M}_k)$ , which offers no help to resolve intractable Bayesian estimation. To relax the complicated full Bayesian model, the approximate,  $Q(\theta|y, \mathcal{M}_k)$  is assigned with a simple structure. VI expresses  $Q(\theta|y, \mathcal{M}_k)$  in a factorized form based on the mean field theorem in physics:

$$Q(\theta|y, \mathcal{M}_k) = \prod q(\theta_i|\mathcal{M}_k). \quad (6)$$

where  $q(\theta_i|\mathcal{M}_k)$  are independent distributions for each element of  $\theta$ . Consequently, problem (5) becomes:

$$Q_{opt}(\theta|y, \mathcal{M}_k) = \arg \max_Q L[Q(\theta|y, \mathcal{M}_k)]$$

subject to:  $Q(\theta|y, \mathcal{M}_k) = \prod q(\theta_i|\mathcal{M}_k)$  (7)

$$\int q(\theta_i|\mathcal{M}_k) d\theta_i = 1, \quad i = 1, 2, \dots$$

By substituting the constraints, the cost function becomes convex with respect to each factor,  $q(\theta_i|\mathcal{M}_k)$ . According to the theory of variational calculus, the solution to the problem is:

$$\ln q(\theta_i|\mathcal{M}_k) = E_{j \neq i} [\ln p(y, \theta)] + c_{\theta_j \neq i}. \quad (8)$$

where the expectation is conducted with respect to the factors,  $q(\theta_j|\mathcal{M}_k)$  ( $j \neq i$ ).  $c_{\theta_j \neq i}$  is a term independent on  $\theta_i$ . Although the set of equations in (8) indicates the consistency conditions of the optimal solution to problem (7), it cannot be solved analytically. To seek for the solution, the factors are updated cyclically following the scheme of the coordinate descent method. Since the cost function is convex, convergence is guaranteed [1].

### 3 MODEL FORMULATION

#### 3.1 The dynamical structure function

The sparse network of  $n$  nodes is described by a linear state space model as follows:

$$x(t+1) = Ax(t) + B_u u(t) + B_e e(t) \quad (9)$$

$$y(t) = Cx(t).$$

where  $x \in \mathcal{R}^n$  are states of the system, each of which represents a node.  $u \in \mathcal{R}^m$  denote inputs.  $y \in \mathcal{R}^p$  present the measurements of the states.  $e \in \mathcal{R}^q$  are i.i.d white Gaussian noise with zero mean and covariance matrix  $P_e$ . Without loss of generality,  $P_e$  is assumed to be diagonal. If the covariance matrix is full, one can decompose the matrix using singular value decomposition (SVD) as  $P_e = R \Sigma R'$ . By replacing  $B_e$  with  $B_e R$ , noise  $e$  have a diagonal covariance,  $\Sigma^{\frac{1}{2}}$ .  $A \in \mathcal{R}^{n \times n}$ ,  $B_u \in \mathcal{R}^{n \times m}$ ,  $B_e \in \mathcal{R}^{n \times q}$  and  $C \in \mathcal{R}^{n \times p}$  are system matrices.

It is normal in practice that some of the nodes are unobservable (hidden states). For example, in a gene regulatory network, the concentration of proteins is usually not measured due to high experimental cost. Therefore, the target of inference is to build a network consisting of measurable nodes. In regard to the gene regulatory network, this means the network is inferred on the transcriptional level.

Assuming the first  $p < n$  states are observable (i.e.  $C = [I, \mathbf{0}]$ ), model (9) is rewritten as follows:

$$\begin{bmatrix} y(t+1) \\ h(t+1) \end{bmatrix} = \begin{bmatrix} A_{11} & A_{12} \\ A_{21} & A_{22} \end{bmatrix} \begin{bmatrix} y(t) \\ h(t) \end{bmatrix} + \begin{bmatrix} B_{u1} \\ B_{u2} \end{bmatrix} u(t) + \begin{bmatrix} B_{e1} \\ B_{e2} \end{bmatrix} e(t), \quad (10)$$

where  $h \in \mathcal{R}^{n-p}$  are hidden states. To avoid inferring hidden states, they are removed from the model. Dynamical structure functions (DSF) encode the information of hidden states via transfer functions [35]:

$$Y = QY + PU + HE. \quad (11)$$

where  $q$  denotes the time shift operator ( $y(t+1) = qy(t)$ ) and:

$$Q = (qI - D)^{-1}(W - D)$$

$$P = (qI - D)^{-1}V_u \quad (12)$$

$$H = (qI - D)^{-1}V_e.$$

with

$$\begin{aligned} W &= A_{11} + A_{12}(qI - A_{22})^{-1}A_{21} \\ V_u &= A_{12}(qI - A_{22})^{-1}B_{u2} + B_{u1} \\ V_e &= A_{12}(qI - A_{22})^{-1}B_{e2} + B_{e1} \\ D &= \text{diag}\{W_{11}, W_{22}, \dots, W_{pp}\}. \end{aligned} \quad (13)$$

$Q$ ,  $P$  and  $H$  are transfer matrices, each element of which is a strictly proper transfer function, indicating that the network is a causal system [34]. Matrix  $Q$  implies the connectivity among observable nodes, whose diagonal elements are zero.  $P$  and  $H$  matrices relate inputs and process noise to nodes, respectively. The topology of the network (i.e. model structure) is reflected by the zero structure of these three matrices. For example, if  $[Q]_{ij}$  is zero, the  $j$ th node does not control the  $i$ th node. Model structures are denoted by  $\mathcal{M}_k$  and  $M_k$  presents the number of links. In particular,  $\mathcal{M}_0$  represents the fully-connected topology. The internal dynamics of the network are described by the transfer functions. The order of a transfer function is relevant to the number of hidden states involved in that regulation pathway.

The input-output map of the network is associated with the DSF as follows:

$$Y = G_u U + G_e E. \quad (14)$$

where

$$\begin{aligned} G_u &= (I - Q)^{-1}P \\ G_e &= (I - Q)^{-1}H. \end{aligned} \quad (15)$$

Ideally, the input-output map can be perfectly recovered based on measurement data. Nevertheless, the corresponding DSF may not be unique, meaning that the network topology is unidentifiable. To ensure the inference problem is well-posed, additional constraints are imposed.

**Proposition 1** (*Identifiability of DSF networks*) [13]

Given a  $p \times (m + q)$  transfer matrix  $G = [G_u, G_e]$ , the DSF is identifiable if and only if  $p - 1$  elements in each column of  $[Q, P, H]'$  are known, which uniquely specifies the component of  $(Q, P, H)$  in the null space of  $[G', I]$ .

A sufficient condition for network identifiability is that matrix  $H$  is diagonal so that  $p - 1$  elements in each column of  $[Q, P, H]'$  are known to be zero. In what follows, we make following assumptions so that no prior knowledge of matrix  $P$  (structure of input channel) is required to guarantee identifiability.

**Assumption 2** *Noise matrix  $H$  is diagonal, monic ( $\lim_{q \rightarrow \infty} qH = I$ ) and minimal phase.*

Stability and sparsity are the basic nature of many practical networks such as biological networks and power systems. Therefore, we assume the target network is stable and sparse.

**Assumption 3** *Transfer matrices,  $Q$  and  $P$  are stable and sparse.*

### 3.2 The likelihood distribution

After simple manipulations, the DSF in (11) can be rewritten as:

$$Y = F_y Y + F_u U + \bar{E}. \quad (16)$$

where

$$F_u = (qH)^{-1}P, \quad F_y = I - (qH)^{-1}(I - Q), \quad \bar{E} = q^{-1}E. \quad (17)$$

Model (16) is a valid causal system. According to the assumptions, transfer matrices,  $F_u$  and  $F_y$  are stable. In addition, since  $H$  is diagonal,  $F_u$  and  $F_y$  have the same zero structure as  $P$  and  $Q$ . As a result,  $F_u$  and  $F_y$  are sparse matrices and imply the network topology.

Identifying model (16) is non-trivial. Since the number of hidden states and the connectivity among them are unknown, estimating the order of the transfer functions requires an exhaustive search of all possible combinations, which is computationally prohibitive for large-scale networks. Additionally, imposing regulations for stable transfer matrices is problematic. To simplify the identification problem, we express model (16) in a non-parametric way. By doing so, the selection of model complexity is avoided and, more importantly, system stability can be promoted effectively. The dynamical system for the  $i$ th target node, is formulated below:

$$\begin{aligned} y_i(t) &= \sum_{j=1}^p \sum_{k=1}^{\infty} h_{ij}^y(k) y_j(t - k) \\ &+ \sum_{j=1}^m \sum_{k=1}^{\infty} h_{ij}^u(k) u_j(t - k) + \bar{e}_i(t). \end{aligned} \quad (18)$$

where  $h_{ij}^y$  and  $h_{ij}^u$  are the impulse responses of transfer functions  $[F_y]_{ij}$  and  $[F_u]_{ij}$ , respectively. The objective is to estimate the impulse responses.

Due to the implementation purpose, the impulse responses are truncated after sample time  $T$ .  $T$  is set sufficiently large in order to catch the major dynamics of the impulse responses (i.e.  $|h(k)| \approx 0$  for  $k \geq T$ ). Assume the availability of time-series data collected from discrete time indices 1 to  $N$  for each node and input. For the  $i$ th target node with  $\mathcal{M}_0$ , we define following matrices and vectors. For other possible model structures,  $\mathcal{M}_k$ , the corresponding terms are defined in the same

way.

$$\begin{aligned}
Y &= \begin{bmatrix} y_i(N) \\ \vdots \\ y_i(T+1) \end{bmatrix}, w = \begin{bmatrix} w_1 \\ \vdots \\ w_{p+m} \end{bmatrix}, \Phi = \begin{bmatrix} \Phi_y & \Phi_u \end{bmatrix} \\
\Phi_y &= \begin{bmatrix} y_1(N-1:N-T) & \cdots & y_p(N-1:N-T) \\ \vdots & \ddots & \vdots \\ y_1(T:1) & \cdots & y_p(T:1) \end{bmatrix} \\
\Phi_u &= \begin{bmatrix} u_1(N-1:N-T) & \cdots & u_m(N-1:N-T) \\ \vdots & \ddots & \vdots \\ u_1(T:1) & \cdots & u_m(T:1) \end{bmatrix} \\
\sigma^{-1} &= E\{\bar{e}_i(t)^2\}.
\end{aligned} \tag{19}$$

where  $Y \in R^{N-T}$  are time-series of the  $i$ th node.  $w \in R^{T(p+m)}$  contain  $p+m$  groups of impulse responses, each of which corresponds to a transfer function of  $F_y$  or  $F_u$ .  $\Phi \in R^{(N-T) \times T(p+m)}$  include time-series of all the nodes and inputs.  $\sigma$  is the noise precision. Note that the dimension of these quantities varies with respect to the model structure.

Based on Bayes' rules, the likelihood distribution of the  $i$ th target node with  $\mathcal{M}_k$  is:

$$p(Y|w, \sigma, D, \mathcal{M}_k) = (2\pi\sigma^{-1})^{-\frac{N-T}{2}} \exp\left\{-\frac{\sigma}{2}\|Y - \Phi w\|_2^2\right\}. \tag{20}$$

where  $D$  denotes the measurements of other nodes and inputs. To simplify the notation,  $D$  is suppressed in the following discussion.

### 3.3 The prior distributions

Full Bayesian treatment deploys prior distributions for each random quantity to build up a hierarchical structure. The prior distributions play a similar role of penalties in regularized optimization problems. They are the key elements to incorporate prior knowledge and impose desired constraints.

Since the impulse responses of model (16) are assumed stable (i.e.  $\sum_{k=1}^{\infty} |h(k)| < \infty$ ), it is necessary to impose regularizations for stability during identification. Kernel machines provides an effective way to construct a functional space as the feasible domain of impulse responses [10]. A reproducing kernel Hilbert space (RKHS) is established using a proper kernel function, which contains stable impulse responses [12]. The impulse responses of the model are estimated by solving a regularized optimization problem in that RKHS. For a SISO system, the problem is formulated as [24]:

$$\arg \min_{h \in \mathcal{H}} \sum_{i=1}^N (y(t_i) - \int_{\mathcal{O}} h(k)y(t_i-k)dk)^2 + \lambda \|h\|_{\mathcal{H}}. \tag{21}$$

where  $y$  is the output of the system.  $h(\cdot)$  are impulse responses.  $\mathcal{H}$  denotes the RKHS of stable impulse responses.  $\|\cdot\|_{\mathcal{H}}$  is the norm of RKHS,  $\mathcal{H}$ .  $\mathcal{O}$  is the time set of the system, which can be discrete or continuous.  $\lambda$  is the weight variable of the penalty.

From the Bayesian perspectives, kernel machines is equivalent to introducing Gaussian processes for impulse responses and solving a maximum a posteriori problem (MAP) [8, 22, 26]. Therefore, we assume the impulse responses of the model are independent Gaussian processes whose covariance functions are Tuned/Correlated kernels (TC kernel). TC kernel has been widely used to characterize stable impulse responses [3]. Other valid kernels include Diagonal/Correlated kernel (DC kernel)<sup>1</sup> and second order stable spline kernel (SS kernel)<sup>2</sup> [12, 23]. The reason why TC kernel is applied in this paper will be explained in the following sections. As a result, the prior distribution for  $w$  is:

$$p(w|\lambda, \beta, \sigma, \mathcal{M}_k) = \prod_{i=1}^{M_k} \mathcal{N}(w_i|0, \sigma^{-1}\lambda_i^{-1}K_i). \tag{22}$$

where  $\beta$  are hyperparameters of TC kernels, which control the exponential decaying rate of impulse responses.  $\lambda$  are scale variables of the kernel functions. In kernel machines, they introduces the effect of Automatic Relevance Determination (ARD) that promotes sparsity estimation [9]. In the Bayesian model,  $\lambda$  influence the probability of model structure (i.e. network topology). As  $\lambda_i$  approaches infinity, distribution  $p(w_i|\lambda_i, \beta_i, \sigma)$  deploys an impulse at the origin, enforcing zero impulse responses. In this case, the  $i$ th node or input does not control the target node. As the standard setting of variational inference, noise precision  $\sigma$  is also used to scale the covariance matrix.  $K_i \in \mathcal{R}^{T \times T}$ ,  $\lambda = [\lambda_1, \dots, \lambda_{M_k}]'$ ,  $\beta = [\beta_1, \dots, \beta_{M_k}]'$  and

$$\begin{aligned}
[K_i]_{ts} &= k(t, s; \beta_i), k(t, s; \beta_i) = \beta_i^{max(t,s)} \\
0 &< \beta_i < 1, \lambda_i \geq 0.
\end{aligned} \tag{23}$$

Since  $\sigma$  is non-negative, a Gamma distribution is assigned as its conjugate prior. Without specific preference on  $\sigma$ , parameters  $a_0$  and  $b_0$  of the distribution are set to 0.001, resulting in a non-informative prior.

$$p(\sigma|a_0, b_0) = Gamma(\sigma|a_0, b_0) = \frac{b_0^{a_0}}{\Gamma(a_0)} \sigma^{a_0-1} e^{-b_0\sigma}. \tag{24}$$

where  $\Gamma(\cdot)$  is the gamma function.

Finally, hyperpriors are assigned to hyperparameters to complete the hierarchy. For hyperparameter  $\lambda_i$ , a

<sup>1</sup>  $k_{DC}(t, s; \beta_1, \beta_2) = \beta_1^{\frac{(t+s)}{2}} \beta_2^{|t-s|}$ ,  $\beta_1 \in (0, 1)$  and  $\beta_2 \in (-1, 1)$

<sup>2</sup>  $k_{SS}(s, t; \beta) = \frac{\beta^{t+s+max(t,s)}}{2} - \frac{\beta^{3max(t,s)}}{6}$ ,  $\beta \in (0, 1)$

Gamma distribution is applied as the conjugate prior. Similar to  $\sigma$ , a non-informative prior is adopted.

$$p(\lambda_i|a_0, b_0) = \text{Gamma}(\lambda_i|a_0, b_0) = \frac{b_0^{a_0}}{\Gamma(a_0)} \lambda_i^{a_0-1} e^{-b_0\lambda_i}. \quad (25)$$

For hyperparameter  $\beta_i$ , a uniform distribution on  $(0, 1)$  is employed as the prior, i.e.,  $p(\beta_i) = 1$ ,  $0 < \beta_i < 1$ .

### 3.4 The full Bayesian model

By incorporating the likelihood and prior distributions, the full Bayesian distribution for model (18) is:

$$\begin{aligned} p(w, \sigma, \lambda, \beta|Y, \mathcal{M}_k) & \propto (2\pi\sigma^{-1})^{-\frac{N-T}{2}} \exp\left\{-\frac{\sigma}{2} \|Y - \Phi w\|_2^2\right\} \\ & \times |2\pi\sigma^{-1}\Lambda^{-1}K| \exp\left\{-\frac{\sigma}{2} w' \Lambda K^{-1} w\right\} \\ & \times \frac{b_0^{a_0}}{\Gamma(a_0)} \sigma^{a_0-1} e^{-b_0\sigma} \times \prod_{i=1}^{M_k} \frac{b_0^{a_0}}{\Gamma(a_0)} \lambda_i^{a_0-1} e^{-b_0\lambda_i}. \end{aligned} \quad (26)$$

where  $K = \text{blkdiag}\{K_1, \dots, K_{M_k}\}$  and  $\Lambda = \text{diag}\{\lambda\} \otimes I_T$ .

### 3.5 Estimation of hyperparameters

Given (26), impulse responses are estimated as the mean of the marginal posterior distribution (i.e.  $p(w|Y) = \int p(w, \sigma, \lambda, \beta|Y) d\sigma d\lambda d\beta$ ). Nevertheless, distribution  $p(w|Y)$  is intractable because the full Bayesian model is highly nonlinear with respect to hyperparameters. Therefore, the estimate of impulse responses cannot be calculated in a closed form.

In the system identification community, deterministic Bayesian approximations have been widely used as the remedy to accommodate non-gaussianity [1]. A candidate distribution,  $p(w)$  is proposed to approximate the marginal distribution,  $p(w|Y)$  analytically. A metric is designed to measure the error between the approximate and the true distributions. The approximate distribution is optimized by minimizing the metric. Finally, the estimate of  $w$  is calculated as the mean of the optimal candidate distribution.

Empirical Bayes and variational inference are two typical methods of deterministic Bayesian approximations whilst empirical Bayes is more prevalent in the kernel-based system identification. The conditional distribution,  $p(w|\lambda, \beta, \sigma, Y)$  is used to approximate the marginal distribution,  $p(w|Y)$ . The hyperparameters are optimized by solving a type II or evidence maximization problem (i.e.  $(\lambda_{opt}, \beta_{opt}, \sigma_{opt}) = \text{argmin}_{\lambda, \beta, \sigma} -\log p(\lambda, \beta, \sigma|Y)$ ). Consequently, the optimal conditional distribution is  $p(w|\sigma_{opt}, \lambda_{opt}, \beta_{opt}, Y)$ . The estimate of  $w$  can be easily calculated as  $\hat{w} = E_{w|\sigma, \lambda, \beta, Y}(w)$  since the logarithm of the conditional distribution is a quadratic function of  $w$  according to (26).

From the view of kernel machines, empirical Bayes provides an effective way to estimate the hyperparameters of kernels whilst problem (21) only solves identification with pre-fixed hyperparameters. This framework has been shown very powerful in exploring system dynamics [21]. Due to the effect of ARD, the estimated  $\lambda$  can also be used for model selection (detection of network topology), leading to sparse networks. The zero structure of  $\lambda^{-1}$  indicates the network topology. Nevertheless, empirical Bayes does not evaluate model evidence,  $p(Y|\mathcal{M}_k)$ . Hence, it is difficult to assess the relative confidence of the estimated model structure over the other possible structures.

Compared with empirical Bayes, the main advantage of VI is that it provides a reasonable approximation of model evidence that is essential for topology detection. VI has been applied to estimate models that can be cast as a sparse linear regression, where it has been shown that VI outperforms empirical Bayes [16] (i.e. sparse Bayesian learning [17, 20, 30, 33]). Nevertheless, VI is much less popular in kernel-based system identification. The updated factors in each iteration no longer have closed-form expressions due to the complex structure of kernel functions, which requests inner sampling loops. In addition, operations of high-dimensional matrices are more involved in this case. In particular, VI have to calculate the inversion and determinant of the ill-conditioned covariance matrix constructed from kernel functions. Nevertheless, by using TC kernel, the computational efficiency and robustness of VI are dramatically improved, which makes VI applicable to practical applications. This paper applies VI to infer sparse networks. Simulations later also show that VI is able to detect network topology accurately.

## 4 VARIATIONAL INFERENCE OF DYNAMICAL STRUCTURE FUNCTIONS

### 4.1 Update of random quantities

For each model structure,  $\mathcal{M}_k$  of (18), the corresponding full Bayesian model,  $p(w, \sigma, \lambda, \beta|Y, \mathcal{M}_k)$  is approximated by a candidate distribution,  $Q(w, \sigma, \lambda, \beta|\mathcal{M}_k)$  using the mean field factorization:

$$Q(w, \sigma, \lambda, \beta|\mathcal{M}_k) = q(w, \sigma|\mathcal{M}_k)q(\lambda|\mathcal{M}_k)q(\beta|\mathcal{M}_k). \quad (27)$$

where  $Q(\cdot)$  and  $q(\cdot)$  are valid probability distributions. Hereafter, the symbol,  $\mathcal{M}_k$  is suppressed to simplify the notation.

The factors of (27) are formulated according to (8). In what follows, the terms independent on the random variables of the factor under consideration are ignored for

convenience. To begin with, factor  $q(w, \sigma)$  is solved as:

$$\begin{aligned} \ln q(w, \sigma) &= E_{\lambda, \beta}[\ln p(y|w, \sigma) + \ln p(w|\sigma, \lambda, \beta)] + \ln p(\sigma) + c_{\lambda, \beta} \\ &= \ln p(y|w, \sigma) + E_{\lambda, \beta}[\ln p(w|\sigma, \lambda, \beta) + \ln p(\sigma)] + c_{\lambda, \beta}. \end{aligned} \quad (28)$$

where

$$\begin{aligned} \ln p(y|w, \sigma) &= \frac{N-T}{2} \ln \sigma - \frac{\sigma}{2} \|Y - \Phi w\|_2^2 \\ E_{\lambda, \beta}[\ln p(w|\sigma, \lambda, \beta)] + \ln p(\sigma) &= \left[ \frac{TM_k}{2} + a_0 - 1 \right] \ln \sigma - \frac{\sigma}{2} w' E_{\lambda}(\Lambda) E_{\beta}(K^{-1}) w - b_0 \sigma. \end{aligned} \quad (29)$$

According to (29), factor  $q(w, \sigma)$  is a Gaussian-Gamma distribution:

$$\begin{aligned} \ln q(w, \sigma) &= \frac{N-T}{2} \ln \sigma - \frac{\sigma}{2} \|Y - \Phi w\|_2^2 \\ &+ \left[ \frac{TM_k}{2} + a_0 - 1 \right] \ln \sigma - \frac{\sigma}{2} w' E_{\lambda}(\Lambda) E_{\beta}(K^{-1}) w - b_0 \sigma \\ &= \ln \mathcal{N}(w|\mu, \sigma^{-1}\Sigma) - \ln \text{Gamma}(\sigma|a^{\sigma}, b^{\sigma}). \end{aligned} \quad (30)$$

where

$$\begin{aligned} \Sigma^{-1} &= \Phi' \Phi + E_{\lambda}(\Lambda) E_{\beta}(K^{-1}), \quad \mu = \Sigma \Phi' Y, \\ a^{\sigma} &= \frac{N-T}{2} + a_0, \quad b^{\sigma} = \frac{1}{2} (Y' Y - \mu' \Sigma^{-1} \mu) + b_0 \\ E_{\sigma, w}(\sigma w w') &= \frac{a^{\sigma}}{b^{\sigma}} \mu \mu' + \Sigma, \quad E_{\sigma, w}(\sigma w) = \frac{a^{\sigma}}{b^{\sigma}} \mu. \end{aligned} \quad (31)$$

Following the same procedure, factor  $q(\lambda)$  is solved as:

$$\begin{aligned} \ln q(\lambda) &= E_{w, \sigma, \beta}[\ln p(w|\sigma, \lambda, \beta) + \ln p(\lambda)] + c_{w, \sigma, \beta} \\ &= E_{w, \sigma, \beta}[\ln p(w|\sigma, \lambda, \beta)] + \ln p(\lambda) + c_{w, \sigma, \beta}. \end{aligned} \quad (32)$$

where

$$\begin{aligned} E_{w, \sigma, \beta}[\ln p(w|\sigma, \lambda, \beta)] &= E \left[ \ln |2\pi\sigma^{-1}\Lambda^{-1}K|^{-\frac{1}{2}} - \frac{\sigma}{2} w' \Lambda K^{-1} w \right] \\ &= \frac{1}{2} \ln |\Lambda| - \frac{1}{2} E_{w, \sigma, \beta} (w' \sigma \Lambda K^{-1} w) \\ &= \frac{1}{2} \ln |\Lambda| - \frac{1}{2} \text{trace} [\Lambda E_{\beta}(K^{-1}) E_{w, \sigma}(\sigma w w')], \\ \ln p(\lambda) &= \sum_{i=1}^{M_k} (a_0 - 1) \ln \lambda_i - b_0 \lambda_i. \end{aligned} \quad (33)$$

Consequently,  $q(\lambda_i)$  are independent Gamma distributions:

$$\begin{aligned} \ln q(\lambda_i) &= \left( \frac{T}{2} + a_0 - 1 \right) \ln \lambda_i \\ &- \lambda_i \left\{ b_0 + \frac{1}{2} \text{trace} \left[ E_{\beta}(K_i^{-1}) \overline{E_{w, \sigma}(\sigma w w')}_i^T \right] \right\} \\ &= \ln \text{Gamma}(\lambda_i | a_{\lambda_i}, b_{\lambda_i}). \end{aligned} \quad (34)$$

where

$$\begin{aligned} a_{\lambda_i} &= \frac{T}{2} + a_0, \quad b_{\lambda_i} = b_0 + \frac{1}{2} \text{trace} \left[ E_{\beta}(K_i^{-1}) \overline{E_{w, \sigma}(\sigma w w')}_i^T \right] \\ E_{\lambda}(\lambda_i) &= \frac{a_{\lambda_i}}{b_{\lambda_i}}. \end{aligned} \quad (35)$$

Finally, factor  $q(\beta)$  is calculated as:

$$\begin{aligned} \ln q(\beta) &= E_{w, \sigma, \lambda}[\ln p(w|\sigma, \lambda, \beta) + \ln p(\beta)] + c_{w, \sigma, \lambda} \\ &= E_{w, \sigma, \lambda}[\ln p(w|\sigma, \lambda, \beta)] + \ln p(\beta) + c_{w, \sigma, \lambda}. \end{aligned} \quad (36)$$

where

$$\begin{aligned} E_{w, \sigma, \lambda}[\ln p(w|\sigma, \lambda, \beta)] &= E \left[ \ln |2\pi\sigma^{-1}\Lambda^{-1}K|^{-\frac{1}{2}} - \frac{\sigma}{2} w' \Lambda K^{-1} w \right] \\ &= -\frac{1}{2} \ln |K| - \frac{1}{2} E_{w, \sigma, \lambda} (w' \sigma \Lambda K^{-1} w) \\ &= -\frac{1}{2} \ln |K| - \frac{1}{2} \text{trace} [E_{\lambda}(\Lambda) K^{-1} E_{w, \sigma}(\sigma w w')] \\ \ln p(\beta) &= 0. \end{aligned} \quad (37)$$

Unlike the other random variables, factor  $q(\beta)$  has no closed-form expression. Nevertheless, the elements of  $\beta$  are independently distributed as:

$$\begin{aligned} q(\beta_i) &= c_i |K_i|^{-\frac{1}{2}} \exp \left\{ -\frac{1}{2} E_{\lambda_i}(\lambda_i) \text{trace} \left[ K_i^{-1} \overline{E_{w, \sigma}(\sigma w w')}_i^T \right] \right\}. \end{aligned} \quad (38)$$

where  $c_i$  is the unknown normalization constant, which cannot be expressed analytically.

#### 4.2 Lower bound of model evidence

Combining all the factors above, the lower bound,  $L[Q(w, \sigma, \lambda, \beta | \mathcal{M}_k)]$  of model evidence  $p(Y | \mathcal{M}_k)$  is:

$$\begin{aligned} L[Q(w, \sigma, \lambda, \beta | \mathcal{M}_k)] &= E[\ln p(Y, w, \sigma, \lambda, \beta)] - E[\ln Q(w, \sigma, \lambda, \beta)] \\ &= E[\ln p(Y|w, \sigma)] + E[\ln p(w|\sigma, \lambda, \beta)] \\ &+ E[\ln p(\sigma, \lambda, \beta)] - E[\ln q(w, \sigma)] \\ &- E[\ln q(\lambda)] - E[\ln q(\beta)]. \end{aligned} \quad (39)$$

where  $\psi(\cdot)$  is the digamma function and:

$$\begin{aligned}
E[\ln p(Y|w, \sigma)] &= \frac{N-T}{2} [\psi(a_\sigma) - \ln b_\sigma] \\
&\quad - \frac{1}{2} \left[ \frac{a_\sigma}{b_\sigma} \|Y - \Phi\mu\|_2^2 + \text{trace}(\Phi\Sigma\Phi') \right]. \\
E[\ln p(w|\sigma, \lambda, \beta)] &= -\frac{1}{2} \sum_{i=1}^{M_k} -T[\psi(a_\sigma) - \ln b_\sigma] - T[\psi(a_{\lambda_i}) - \ln b_{\lambda_i}] \\
&\quad - \frac{1}{2} \sum_{i=1}^{M_k} \frac{a_{\lambda_i}}{b_{\lambda_i}} \text{trace} \left[ E(K_i^{-1}) \overline{\left( \frac{a_\sigma}{b_\sigma} \mu\mu' + \Sigma \right)_i^T} \right]. \\
E[\ln p(\lambda, \beta)] &= \sum_{i=1}^{M_k} a_0 \ln b_0 - \ln \Gamma(a_0) \\
&\quad + \sum_{i=1}^{M_k} (a_0 - 1) [\psi(a_{\lambda_i}) - \ln b_{\lambda_i}] - b_0 \frac{a_{\lambda_i}}{b_{\lambda_i}}. \\
E[\ln p(\sigma)] &= a_0 \ln b_0 - \ln \Gamma(a_0) \\
&\quad + (a_0 - 1) [\psi(a_\sigma) - \ln b_\sigma] - b_0 \frac{a_\sigma}{b_\sigma}. \\
E[\ln q(w, \sigma)] &= \frac{TM_k}{2} [\psi(a_\sigma) - \ln b_\sigma] - \frac{1}{2} \ln |\Sigma| - \frac{TM_k}{2} \\
&\quad + a_\sigma \ln b_\sigma - \ln \Gamma(a_\sigma) + (a_\sigma - 1) [\psi(a_\sigma) - \ln b_\sigma] - a_\sigma. \\
E[\ln q(\beta)] &= \sum_{i=1}^{M_k} \ln c_i - \frac{1}{2} \sum_{i=1}^{M_k} E \ln |K_i| \\
&\quad + E(\lambda_i) \text{trace} \left[ E(K_i^{-1}) \overline{\left( \frac{a_\sigma}{b_\sigma} \mu\mu' + \Sigma \right)_i^T} \right]. \\
E[\ln q(\lambda)] &= \sum_{i=1}^{M_k} a_{\lambda_i} \ln b_{\lambda_i} - \ln \Gamma(a_{\lambda_i}) \\
&\quad + \sum_{i=1}^{M_k} (a_{\lambda_i} - 1) (\psi(a_{\lambda_i}) - \ln b_{\lambda_i}) - a_{\lambda_i}.
\end{aligned} \tag{40}$$

Finally, the lower bound is:

$$\begin{aligned}
L[Q(w, \sigma, \lambda, \beta | \mathcal{M}_k)] &= \frac{1}{2} \ln |\Sigma| - b_0 \frac{a_\sigma}{b_\sigma} - \frac{1}{2} \left[ \frac{a_\sigma}{b_\sigma} \|Y - \Phi\mu\|_2^2 + \text{trace}(\Phi\Sigma\Phi') \right] \\
&\quad - a_\sigma \ln b_\sigma - \sum_{i=1}^{M_k} a_{\lambda_i} \ln b_{\lambda_i} + \frac{TM_k}{2} \\
&\quad + M_k [a_0 \ln b_0 - \ln \Gamma(a_0) + \ln \Gamma(a_{\lambda_i})] \\
&\quad - \sum_{i=1}^{M_k} b_0 \frac{a_{\lambda_i}}{b_{\lambda_i}} - a_{\lambda_i} + \ln c_i.
\end{aligned} \tag{41}$$

where the constant terms independent on  $\mathcal{M}_k$  are ignored.

### 4.3 Algorithm for variational inference

Unfortunately, factors  $q(w, \sigma)$ ,  $q(\lambda)$  and  $q(\beta)$  cannot be solved analytically. Hence, they are calculated cyclically in each iteration of the algorithm. Each factor is updated based on the newest update of the other factors in the current iteration. The procedure is summarized in Algorithm 1.

---

#### Algorithm 1 Variational inference of DSF

---

- 1: Initialize  $\mu, \Sigma, a_\sigma, b_\sigma, a_{\lambda_i}, b_{\lambda_i}$  and  $E_\beta(K^{-1})$
- 2: **for**  $k = 1 : \text{Max do}$
- 3: Update  $q(w, \sigma)$  as a Gaussian-Gamma distribution:

$$\begin{aligned}
\Sigma^{-1} &= \Phi' \Phi + E_\lambda(\Lambda) E_\beta(K^{-1}) \\
\mu &= \Sigma \Phi' Y \\
a^\sigma &= \frac{N-T}{2} + a_0 \\
b^\sigma &= \frac{1}{2} (Y' Y - \mu' \Sigma^{-1} \mu) + b_0
\end{aligned} \tag{42}$$

- 4: Update  $q(\lambda)$  as a Gamma distribution:

$$\begin{aligned}
a_{\lambda_i} &= \frac{T}{2} + a_0 \\
b_{\lambda_i} &= \frac{1}{2} \text{trace} \left[ E_{\beta_i}(K_i^{-1}) \overline{\left( \frac{a_\sigma}{b_\sigma} \mu\mu' + \Sigma \right)_i^T} \right]
\end{aligned} \tag{43}$$

$$E(\lambda_i) = \frac{a_{\lambda_i}}{b_{\lambda_i}}$$

- 5: Update  $q(\beta_i)$  and  $E_{\beta_i}(K_i^{-1})$  according to:

$$\begin{aligned}
q(\beta_i) &= c_i |K_i|^{-\frac{1}{2}} \exp \left\{ -\frac{a_{\lambda_i}}{2b_{\lambda_i}} \text{trace} \left[ K_i^{-1} \overline{\left( \frac{a_\sigma}{b_\sigma} \mu\mu' + \Sigma \right)_i^T} \right] \right\}
\end{aligned} \tag{44}$$

- 6: Update the lower bound,  $L[Q]$  of model evidence according to (41).

- 7: **if**  $L[Q]_k - L[Q]_{k-1} < \epsilon$  **then**

- 8: Break

- 9: **end if**

- 10: **end for**

- 11: Estimate  $w$  as  $\hat{w} = \mu$  and store  $L[Q]$  for topology detection
- 

In Algorithm 1, term  $E(K^{-1})$  is estimated in each iteration. However, Since  $q(\beta)$  is only known up to a normalization constant,  $E(K^{-1})$  cannot be calculated analytically. Hence, numerical sampling methods are used to estimate the expectation. Since hyperparameters  $\beta_i \in (0, 1)$  are independently distributed, they can be sampled in parallel. We use the Metropolis-Hastings sampling method to draw samples from (38). A uniform distribution is applied as the proposal distribution for  $\beta_i$ . Let  $\hat{p}(\beta_i) = |K_i|^{-\frac{1}{2}} \exp\{-\frac{a_{\lambda_i}}{2b_{\lambda_i}} \text{trace}[K_i^{-1} \overline{(\frac{a_\sigma}{b_\sigma} \mu\mu' + \Sigma)_i^T}]\}$ . At current

state  $\beta_i^k$ , a proposal  $\beta_i^p$  is drawn from:

$$q_p(\beta_i^p|\beta_i^k) = \begin{cases} U(\beta_i^t - \frac{\varepsilon}{2}, \beta_i^t + \frac{\varepsilon}{2}) & \frac{\varepsilon}{2} < \beta_i^k < 1 - \frac{\varepsilon}{2} \\ U(0, \varepsilon) & \frac{\varepsilon}{2} \geq \beta_i^k \\ U(1 - \varepsilon, 1) & 1 - \frac{\varepsilon}{2} \leq \beta_i^k \end{cases} \quad (45)$$

where  $U(a, b)$  is the uniform distribution on  $(a, b)$ .  $\varepsilon$  is the selection window for sampling, which is set to 0.1. The acceptance ratio is  $r(\beta_i^p|\beta_i^k) = \min\{1, \frac{\hat{p}(\beta_i^p)q_p(\beta_i^k|\beta_i^p)}{\hat{p}(\beta_i^k)q_p(\beta_i^p|\beta_i^k)}\}$ . If the proposal is accepted,  $\beta_i^{k+1} = \beta_i^p$ . Otherwise,  $\beta_i^{k+1} = \beta_i^k$ . With  $N$  samples  $\{\beta_i^k|k = 1, \dots, N\}$ ,  $E(K_i^{-1})$  is estimated as  $E(K_i^{-1}) = \frac{1}{N} \sum_{k=1}^N (K_i^k)^{-1}$ .

In addition, in order to calculate the lower bound of model evidence, one has to estimate the normalization constant,  $c_i$  of  $q(\beta_i)$  in (38). Since  $\beta_i$  is a scalar on  $(0, 1)$ , numeric integration methods (e.g. adaptive quadrature [29]) are sufficient to give an accurate estimation based on  $c_i^{-1} = \int \hat{p}(\beta_i)d\beta_i$ .

#### 4.4 Algorithm implementation

The algorithm requires to calculate the inversion and determinant of the covariance matrix,  $K_i$  in each iteration. These two operations are computationally heavy because  $K_i$  is a full matrix, and its inversion and determinant must be calculated thousands of times in the sampling loop of  $\beta_i$  per iteration, depending on the number of samples required. With standard methods, they both demand  $O(T^3)$  work. More importantly,  $K_i$  may be ill-conditioned if the hyperparameters of the kernel functions are close to 0, causing numerical instability during implementation [7]. These issues may occur for all three kernels (i.e. TC, DC and SS kernels). Therefore, it is necessary to find a robust and efficient way to deal with matrix operations.

It has been shown that the covariance matrix constructed using the TC or DC kernel can be decomposed analytically whilst that of the SS kernel cannot [4, 6]. As a result, SS kernel is not adopted in our VI framework. Rather, TC kernel that possesses the simplest structure is applied to improve the robustness and to reduce the computational cost of the algorithm. The inverse covariance matrix,  $K^{-1} \in \mathcal{R}^{T \times T}$  constructed using TC kernel (i.e.  $[K]_{ts} = k(t, s; \beta)$ ) can be decomposed as [3]:

$$K^{-1} = U'WU. \quad (46)$$

where  $U$  is an upper triangular matrix and  $W$  is a diagonal

matrix as follows:

$$U = \begin{bmatrix} 1 & -1 & \cdots & 0 \\ 0 & \ddots & \ddots & \vdots \\ \vdots & 0 & \ddots & -1 \\ 0 & \cdots & 0 & 1 \end{bmatrix}$$

$$W = (1 - \beta)^{-1} \text{diag}\{\beta^{-1}, \beta^{-2}, \dots, \beta^{-T+1}, \frac{1 - \beta}{\beta^T}\}. \quad (47)$$

Consequently, matrix inversion only demands  $O(T)$  work considering the sparse structure of  $U$  and  $W$  whilst matrix determinant ( $|K| = \beta^{\frac{T(T+1)}{2}}(1 - \beta)^{T-1}$ ) requires  $O(1)$ . With  $N$  samples of  $\beta$  ( $\{\beta^k|k = 1, \dots, N\}$ ), the expectation of the inverse matrix costs  $O(NT)$  work:

$$E(K^{-1}) = \frac{1}{N} U' \left[ \sum_{k=1}^N W^k \right] U. \quad (48)$$

#### 4.5 Detection of network topology

Hyperparameter  $\lambda^{-1}$  are ARD variables, whose zero structure determines the network topology. Nevertheless, due to local optimal solutions and numerical errors, none of these estimated variables are exactly zero in practical implementation. To improve the inference accuracy, the backward selection method is used for model selection.

Model selection is based on the posterior distribution of model structures (i.e.  $p(\mathcal{M}_k|y) \propto p(y|\mathcal{M}_k)p(\mathcal{M}_k)$ ). Assuming equal probability for each model structure, the distribution is proportional to model evidence,  $p(\mathcal{M}_k|y) \propto p(y|\mathcal{M}_k)$ . The by-product of VI provides a lower bound of model evidence, which can be used to determine the most probable model structure (network topology). Nevertheless, the complete evaluation of model evidence requires an exhaustive search of all possible model structures, which is computationally prohibitive for large-scale networks. To tackle this problem, we come up with a heuristic strategy that applies backward selection to reduce the computational burden. The resulting cost of topology detection grows linearly with respect to the scale of the network.

To begin with, VI is conducted to infer a fully-connected network (i.e.  $\mathcal{M}_0$ ). The confidence of inferred links is measured by the norm of their impulse responses. These links are removed from the model one-by-one, each time producing a particular model structure. The VI algorithm is implemented repeatedly with the proposed model structures until the network becomes empty. The best model structure is determined according to the highest lower bound of model evidence. The above procedure is summarized in Algorithm 2.

---

**Algorithm 2** Variational inference of network topology

---

- 1: Implement Algorithm 1 with model structure  $\mathcal{M}_0$ .
  - 2: Set the threshold  $R = asc\{\|w_1\|, \dots, \|w_{n+p}\|\}$ .
  - 3: **for**  $k=1:n+p-1$  **do**
  - 4:    $I = \{i \mid \|w_i\| \leq R_k\}$
  - 5:   Remove the links in index set  $I$ , producing  $\mathcal{M}_k$
  - 6:   Run Algorithm 1 with  $\mathcal{M}_k$
  - 7: **end for**
  - 8:  $\mathcal{M}_{opt} = argmax_{\mathcal{M}_k} L[Q(w, \sigma, \lambda, \beta | \mathcal{M}_k)]$
- 

## 5 SIMULATION

We conducted Monte Carlo simulations and compared our method with another kernel-based system identification approach. The state-of-art method applies empirical Bayes to estimate hyperparameters and to detect network topology, where DC (Kernel\_DC), SS (Kernel\_SS) and TC (Kernel\_TC) kernels were all used for inference. KEB solves the optimization problem as follows. More details can be found in [9].

$$\arg \min_{\sigma, \gamma, \beta} Y'(\sigma I + \Phi \Gamma K \Phi')^{-1} Y + \ln |\sigma I + \Phi \Gamma K \Phi'|, \quad (49)$$

where  $\Gamma$  is equivalent to  $\Lambda^{-1}$  in our framework.  $K$  is the covariance matrix constructed by kernel functions. If  $\gamma_i$  is 0, the  $i$ th node does not control the target node. To select the inferred links, a similar backward selection method is used [9].

The DSF networks for test were generated randomly with diverse topologies (including an extremely sparse type, a ring structure), simulated under various noise levels and inferred using time-series data of different length.

Two criteria are applied to evaluate the performance of algorithms, namely True Positive Rate (TPR) and Precision (PREC). TPR shows the percentage of the true links in the ground truths that were successfully inferred. TPR implies the information richness of the inference result. PREC equates to the rate of the correct links over the all inferred. PREC indicates the reliability or accuracy of the inferred network. Hence, ensuring a high PREC is the first priority in real applications. If, for example, PREC is below 50%, one cannot tell which inferred links are correct. To investigate whether the inferred networks have internal dynamics consistent with the ground truths, the estimated models were simulated to predict the validation dataset that was not used for inference. The prediction accuracy is measured based on the metric as follows.

$$fitness = 100 \left( 1 - \frac{\|y - \hat{y}\|}{y - \bar{y}} \right) \quad (50)$$

where  $y$  are the validation data of a certain node,  $\hat{y}$  are the predicted output and  $\bar{y}$  are the mean of the validation data. The fitness of all nodes was averaged to generate the conclusion.

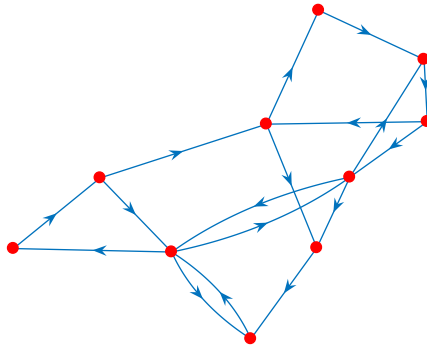


Fig. 1. The structure of a randomly generated network. Solid lines with arrows represent links. Red circles denote nodes.

### 5.1 Random DSF networks

100 networks were generated with random topologies and internal dynamics. All networks contained 15 nodes in total. Each node was independently driven by an input that is known and process noise that is assumed to be unknown during inference. DSF models were produced from state space models (9). To be specific, a sparse stable matrix  $A \in \mathcal{R}^{15 \times 15}$  was first yielded randomly using the function *sprandn*( $n, n, density$ ) in Matlab. The brute force strategy was applied to guarantee that matrix  $A$  was Hurwitz (that is, no eigenvalue was outside the unit circle of the complex plane) and that no isolated nodes existed in the network.

To simulate the models, inputs and process noise were both i.i.d. white Gaussian signals. The variance of inputs was fixed to 1 whilst that of process noise varied. The Signal-to-Noise ratio is defined as  $SNR = 10 \log \frac{\sigma_u}{\sigma_e}$  where  $\sigma_u$  and  $\sigma_e$  are signal variance of inputs and noise, respectively. The first 10 states of the models were measured, leaving the rest 5 as hidden nodes. Figure 1 displays one example of the resulting networks. The length of impulse responses after truncation was set to 20. The data for inference were collected with different length.

The average TPR and PREC over 100 trials are recorded in Table 1-3. In the best-case scenario (no noise), VI outperforms all the other methods. In particular, almost all the inferred links of VI are correct ( $PREC \approx 100\%$ ), regardless of the number of data points. Meanwhile, VI is able to identify most true links of the ground truths.

With 100 data points, VI recovers the network perfectly. In contrast, Kernel\_TC presents the weakest result. PREC of Kernel\_TC stays low unless more data points are available for inference. The poor performance of Kernel\_TC indicates the effectiveness of VI that uses the same kernel function.

As  $SNR$  decreases to  $10dB$ , all methods require more data points to counteract the interference of process noise. Although TRP of VI is slightly lower than Kernel\_SS, PREC of VI is much higher than Kernel\_SS,

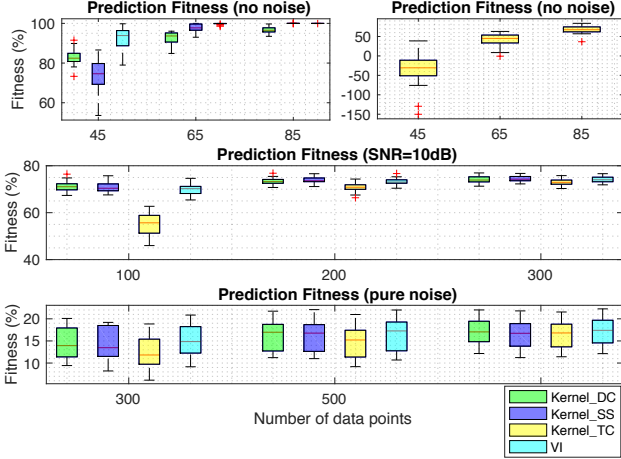


Fig. 2. Prediction of randomly generated networks.

which is close to 100%. Kernel\_TC also achieves accurate results. Nevertheless, many true links are missed ( $TPR < 80\%$ ).

It is remarkable that the inferred networks of VI are highly reliable ( $PREC \approx 100\%$ ) even under the worst-case scenario (that of pure noise). The lack of data points only affects TPR of VI whilst PREC remains high. The gap of TPR between Kernel\_SS and VI decreases gradually as more data points are available. Similar to the above cases, Kernel\_TC is outperformed by VI. Based on the simulations, VI presents great advantages on inference accuracy over the other methods. Almost all the inferred links of VI are correct regardless of the noise level and number of data points. Generally, TPR of VI is slightly lower than Kernel\_SS. However, VI actually missed only a few more true links compared with Kernel\_SS since the target networks were sparse. On average, there were 18.25 links per network in the simulations. According to the results, VI, at most missed, 2.7 links more than Kernel\_SS.

The validation result is shown by the box plot in Figure 2. With negligible process noise, VI clearly outperforms all the other methods. The prediction fitness of VI is above 80% and reaches approximately 100%, given enough data. As  $SNR$  decreases to 10dB, all methods, except Kernel\_TC present similar performance. When process noise overwhelms inputs, the prediction fitness of all methods drops seriously to below 30%. In this case, the performance of VI is slightly better than the others. Note that Kernel\_TC presents the weakest result under different noise levels, implying that VI is able to improve the performance of empirical Bayes at least with TC kernel.

## 5.2 Ring networks

100 networks with the fixed ring structure as shown in Figure 3 were generated and simulated following the same protocol in the last section. Each node was driven

Table 1  
Inference of random networks with no noise

	No Noise					
	45		65		85	
	PREC	TPR	PREC	TPR	PREC	TPR
Kernel_DC	94.3	56.9	97.7	73.1	97.9	85.2
Kernel_SS	84.7	58.3	91.4	91.7	100	100
Kernel_TC	43.3	16.5	71.1	23.4	98.3	42.9
VI	100	75.0	99.7	98.5	100	100

Table 2  
Inference of random networks with 10dB SNR

	10dB					
	100		200		300	
	PREC	TPR	PREC	TPR	PREC	TPR
Kernel_DC	95.6	77.1	98.6	84.2	96.5	86.9
Kernel_SS	74.1	82.5	79.7	88.3	86.3	91.0
Kernel_TC	92.5	46.5	100	66.2	99.6	75.7
VI	100	68.2	99.7	81.3	100	86.4

Table 3  
Inference of random networks with pure noise

	No Input					
	300		500		1000	
	PREC	TPR	PREC	TPR	PREC	TPR
Kernel_DC	77.6	72.9	89.1	75.6	96.9	79.1
Kernel_SS	64.3	69.6	81.7	76.1	88.0	77.1
Kernel_TC	77.9	60.3	87	65.7	93.4	70.9
VI	100	56.5	100	65.0	100	74.9

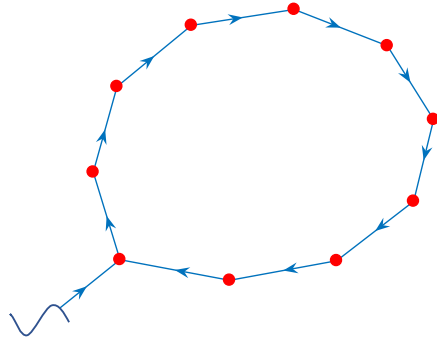


Fig. 3. A network with the ring structure. Symbol '~' denotes the input signals.

by independent process noise. Only one input entered the network through a single node. Since the network contains a feedback loop and is extremely sparse, it is more challenging to infer.

Table 4 presents the inference result. VI is still able to produce reliable networks with the highest PREC among all the methods ( $PREC = 100\%$ ). More importantly, PREC of the other three cases highly relies on the number of data points whilst that of VI does not. TPR of VI and Kernel\_SS are very close. Since the ring network contained only 10 links, VI at most missed 3 true links.

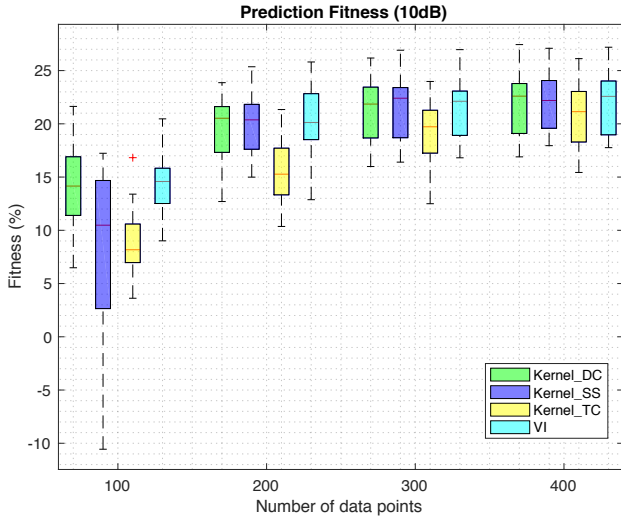


Fig. 4. Prediction of ring networks.

Simulations indicate that VI is able to provide reliable inference results and identify most true links of the ground truths even if the target networks are extremely sparse. More importantly, the performance of VI is robust ( $PREC \approx 100\%$ ), which is crucial in real applications where the measurements are not sufficient for inference.

The validation result is shown in Figure 4. Since the ring network was mostly driven by process noise, the prediction fitness of all methods is below 30%. The prediction accuracy of VI is competitive with Kernel\_DC. Kernel\_TC presents the weakest result, which implies that VI improves the performance of KEB.

Table 4  
Inference of ring networks with 10dB SNR

	10dB							
	100		200		300		400	
	PREC	TPR	PREC	TPR	PREC	TPR	PREC	TPR
Kernel_DC	51.0	75.0	75.8	81.0	86.2	84.0	93.8	84.5
Kernel_SS	42.2	76.5	64.2	83.5	67.8	86.5	74.6	88.5
Kernel_TC	76.9	19.3	99.3	32.5	97.3	55.0	98.5	68.5
VI	100	27.5	100	66.0	100	73.5	100	80.0

## 6 CONCLUSION AND DISCUSSION

This paper has applied variational inference to identify DSF models given measured time series data. No prior knowledge of the hidden nodes including their number and internal connectivity is required. Both the system dynamics and topology of sparse linear network can be inferred accurately. The proposed method achieves this by incorporating kernel-based methods to promote system stability and by introducing VI to imposing network sparsity. By decomposing the kernel function, the resulting algorithm becomes computationally efficient and robust. Monte Carlo simulations imply that our method always produces reliable inference result regardless of challenging experimental conditions (for exam-

ple, lower number of data points, high levels of noise, and extremely sparse topologies). The inference of links is highly accurate (with nearly 100% confidence): only a few true links are missed. Therefore, the developed method appears highly reliable for real-world applications.

Overall, the value of this approach is that the performance of KEB is greatly improved, at least in regard to TC kernel. Our method raises the reliability of inference results to the highest level (100%  $PREC$ ). In particular, our method is applicable to real-world networks where full state measurements are normally unavailable such as gene regulatory networks. The estimated DSF models can be used for simulation and prediction by the virtue of system stability.

The performance of our method may be further improved using other kernel functions (e.g. DC and SS). However, the computational cost of doing so is heavy and the robustness of the algorithm is not guaranteed.

Future developments should include two aspects. The first is to find an effective decomposition for the SS covariance matrix so that SS kernel can be used in our framework. The second aspect is to further improve TPR of inferred networks while maintaining high  $PREC$ . Considering most real-world networks are nonlinear, it is necessary to extend our framework to black-box nonlinear systems.

## References

- [1] C. Bishop. *Pattern recognition and machine learning*. Springer New York, 2006.
- [2] D. M. Blei, A. Kucukelbir, and J. D. McAuliffe. Variational inference: A review for statisticians. *Journal of the American Statistical Association*, 112(518):859–877, 2017.
- [3] G. Bottegal, A. Y. Aravkin, H. Hjalmarsson, and G. Pillonetto. Robust em kernel-based methods for linear system identification. *Automatica*, 67:114 – 126, 2016.
- [4] F. P. Carli, T. Chen, and L. Ljung. Maximum entropy kernels for system identification. *IEEE Transactions on Automatic Control*, 62(3):1471–1477, March 2017.
- [5] T. Chen, M.S. Andersen, L. Ljung, A. Chiuso, and G. Pillonetto. System identification via sparse multiple kernel-based regularization using sequential convex optimization techniques. *Automatica*, 59(11):1–33, 2014.
- [6] T. Chen, T. Ardeshiri, F. P. Carli, A. Chiuso, L. Ljung, and G. Pillonetto. Maximum entropy properties of discrete-time first-order stable spline kernel. *Automatica*, 66:34 – 38, 2016.
- [7] T. Chen and L. Ljung. Implementation of algorithms for tuning parameters in regularized least squares problems in system identification. *Automatica*, 49(7):2213 – 2220, 2013.
- [8] T. Chen, H. Ohlsson, and L. Ljung. On the estimation of transfer functions, regularizations and gaussian processes-revisited. *Automatica*, 48(8):1525 – 1535, 2012.
- [9] A. Chiuso and G. Pillonetto. A Bayesian approach to sparse dynamic network identification. *Automatica*, pages 1553–1565, 2012.
- [10] F. Cucker and S. Smale. On the mathematical foundations of learning. *Bulletin of the American Mathematical Society*, 39:1–49, 2002.

- [11] M. Darwish, P. Cox, G. Pillonetto, and R. Tth. Bayesian identification of lpv box-jenkins models. In *2015 54th IEEE Conference on Decision and Control (CDC)*, pages 66–71, Dec 2015.
- [12] F. Dinuzzo. Kernels for linear time invariant system identification. *SIAM Journal on Control and Optimization*, 53(5):3299–3317, 2015.
- [13] J. Gonçalves and S. Warnick. Necessary and sufficient conditions for dynamical structure reconstruction of lti networks. *IEEE Trans. Automat. Contr.*, 53(7):1670–1674, 2008.
- [14] A. Graves. Practical variational inference for neural networks. In J. Shawe Taylor, R. S. Zemel, P. L. Bartlett, F. Pereira, and K. Q. Weinberger, editors, *Advances in Neural Information Processing Systems 24*, pages 2348–2356. Curran Associates, Inc., 2011.
- [15] M. Hoffman, D.M. Blei, C. Wang, and J. Paisley. Stochastic Variational Inference. *ArXiv e-prints*, June 2012.
- [16] W. R. Jacobs, T. Baldacchino, T. J. Dodd, and S. R. Anderson. Sparse bayesian nonlinear system identification using variational inference. *IEEE Transactions on Automatic Control*, pages 1–1, 2018.
- [17] J. Jin, Y. Yuan, W. Pan, C. Tomlin, A. A. Webb, and J. Gonçalves. Identification of nonlinear sparse networks using sparse bayesian learning. In *2017 IEEE 56th Annual Conference on Decision and Control (CDC)*, pages 6481–6486, Dec 2017.
- [18] A. Mnih and K. Gregor. Neural Variational Inference and Learning in Belief Networks. *ArXiv e-prints*, January 2014.
- [19] Kevin P. Murphy. *Machine Learning: A Probabilistic Perspective*. The MIT Press, 2012.
- [20] W. Pan, Y. Yuan, J. Gonçalves, and G. Stan. A sparse bayesian approach to the identification of nonlinear state-space systems. *IEEE Transactions on Automatic Control*, 61(1):182–187, Jan 2016.
- [21] G. Pillonetto and A. Chiuso. Tuning complexity in regularized kernel-based regression and linear system identification: The robustness of the marginal likelihood estimator. *Automatica*, 58:106 – 117, 2015.
- [22] G. Pillonetto, A. Chiuso, and G.D. Nicolao. Prediction error identification of linear systems: A nonparametric gaussian regression approach. *Automatica*, 47(2):291 – 305, 2011.
- [23] G. Pillonetto, F. Dinuzzo, T. Chen, G. De Nicolao, and L. Ljung. Kernel methods in system identification, machine learning and function estimation: A survey. *Automatica*, 50(3):657–682, 2014.
- [24] G. Pillonetto and G. De Nicolao. A new kernel-based approach for linear system identification. *Automatica*, 46(1):81–93, 2010.
- [25] G. Pillonetto, M. H. Quang, and A. Chiuso. A new kernel-based approach for nonlinear system identification. *IEEE Transactions on Automatic Control*, 56(12):2825–2840, Dec 2011.
- [26] C. E. Rasmussen and C. K. I. Williams. *Gaussian processes for machine learning*. The MIT Press, 2006.
- [27] R. S. Risuleo. *System Identification with input uncertainties: an EM kernel-based approach*. PhD thesis, KTH of School of Electrical Engineering, 2016.
- [28] R. S. Risuleo, G. Bottegal, and H. Hjalmarsson. Kernel-based system identification from noisy and incomplete input-output data. In *2016 IEEE 55th Conference on Decision and Control (CDC)*, pages 2061–2066, Dec 2016.
- [29] L.F. Shampine. Vectorized adaptive quadrature in matlab. *Journal of Computational and Applied Mathematics*, 211(2):131 – 140, 2008.
- [30] M. Tipping. Sparse Bayesian learning and the relevance vector machine. *J. Mach. Learn. Res.*, 1:211–244, 2001.
- [31] M. K. Titsias and L.G. Miguel. Spike and slab variational inference for multi-task and multiple kernel learning. In J. Shawe-Taylor, R. S. Zemel, P. L. Bartlett, F. Pereira, and K. Q. Weinberger, editors, *Advances in Neural Information Processing Systems 24*, pages 2339–2347. Curran Associates, Inc., 2011.
- [32] M. J. Wainwright and M. I. Jordan. Graphical models, exponential families, and variational inference. *Found. Trends Mach. Learn.*, 1(1-2):1–305, January 2008.
- [33] D.P. Wipf, B.D. Rao, and S. Nagarajan. Latent variable Bayesian models for promoting sparsity. *IEEE Trans. Inf. Theory.*, 57(9):6236–6255, 2011.
- [34] Y. Yuan, A. Rai, E. Yeung, G. Stan, S. Warnick, and J. Gonçalves. A minimal realization technique for the dynamical structure function of a class of lti systems. *IEEE Transactions on Control of Network Systems*, 4(2):301–311, June 2017.
- [35] Y. Yuan, G. Stan, S. Warnick, and J. Gonçalves. Robust dynamical network structure reconstruction. *Automatica*, 47:1230–1235, 2011.